An Investigation of the Magnitude and Causes of Count Loss Artifacts in SPECT Imaging

Gerard J. Gillen, Brian Gilmore, and Alex T. Elliott

West of Scotland Health Boards, Department of Clinical Physics and Bio-Engineering, Glasgow, Scotland and Medical Physics Department, Belvoir Park Hospital, Belfast, Ireland

A quantitative evaluation and an investigation of the mechanism of the count losses that can occur in SPECT imaging is described. The most common clinical example of the artifacts which result from this is encountered when sections are taken through the femoral heads in skeletal studies of the pelvis. From some simple phantom studies, it was identified that the count losses were associated with the presence of a high dynamic range in the projection data. Further information was obtained from simulation studies. It was found that the count loss phenomenon is caused by the combined effects of the presence of a high count density area and a structure with a relatively high attenuation level. An appreciation of the presence, magnitude, and mechanism of this effect is important if erroneous clinical findings are to be avoided. This is particularly relevant because of the existence of a variety of techniques that can be used to remove the resulting artifacts.

J Nucl Med 1991; 32:1771–1776

Skeletal imaging using SPECT has been shown to be of use for the investigation of avascular necrosis of the femoral heads (*1*). Unfortunately, it is common for 20% or more investigations to be of no value due to the creation of artifacts which are associated with the presence of high and changing levels of activity within the bladder (*2*).

The most obvious type of artifact takes the form of streaks which can extend across the whole width of a transaxial section. The formation of this type of artifact is well known as is its cause, the inconsistent nature of the projection data due to the changes in bladder activity over the duration of the study acquisition (*3*). This effect is exacerbated by inadequate angular sampling.

However, another form of artifact may also be present in many studies. This appears as a reduction in counts in structures in the same axial plane as the bladder and occurs if the activity in the bladder is high (Fig. 1). When coronal sections are taken through the hips, the count losses in the femoral heads can easily be mistaken for the photon-deficient areas that are diagnostic of femoral head avascular necrosis (*3*).

Received Oct. 11, 1990; revision accepted Mar. 19, 1991.

For reprints contact: Dr. Gerard J Gillen, Department of Clinical Physics and Bio-Engineering, 11 West Graham St., Glasgow G4 91F, Scotland.

To investigate and quantify this phenomenon some simple phantom and simulation studies were performed.

METHODS

Phantom Studies

To represent the bladder and a femoral head, two cylindrical containers 11 cm in length and 6 cm in diameter were used. The phantom were aligned with their long axes parallel to and equidistant from the axis of rotation and separated by a center to center distance of 12 cm.

The container representing the femoral head was filled to give a concentration of ^{99m}Tc which would give similar count densities to those found in the femoral heads during clinical studies. The bladder phantom was filled with a variety of concentrations of ^{99m}Tc chosen to give activity ratios of from 0 to 50 times that in the femoral head phantom. A separate SPECT acquisition was performed for each bladder-to-femoral head phantom activity ratio. The total activity in both phantoms was such that the count rate was always below 5,000 cps, ensuring that count rate losses did not occur.

SPECT acquisitions were performed with a radius of rotation of 20 cm using 64 angles over 360° with pixels of edge length 0.7 cm. The camera used was the Siemens Orbiter.

The SPECT data were reconstructed by filtered backprojection with a Shepp-Logan filter. The computing system used was a Bartec Systems Micas 3, which is a 16-bit microcomputer.

To reduce the effects of statistical noise, 10 transaxial sections along the center of each cylinder were summed. Identical, square regions of interest were drawn inside the center of the bladder and femoral head phantoms and the counts determined in each for the set of bladder-to-femoral head phantom activity ratios.

The exact values of the bladder-to-femoral head phantom activity ratios were determined from conventional planar images which were also taken.

Simulation Studies

To investigate the precise mechanism of the count loss phenomenon some simulation studies were performed.

First, an analytical calculation of the projection data which would result from the tomographic acquisition of two uniform count density disks was made. To match the phantom studies the calculation was performed using 64 projection angles spaced over 360° and with pixels of edge length 0.7 cm. The reconstructions were performed using a Shepp-Logan filter. The disks were 6 cm in diameter and separated by a center-to-center distance of 12 cm. One disk was chosen to represent the femoral head and the other the bladder. The count densities in the femoral head

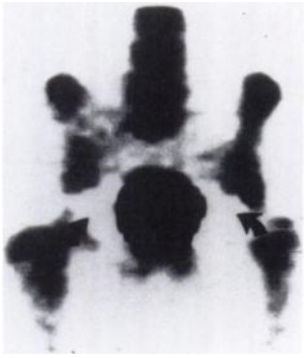

FIGURE 1. Coronal section through normal femoral heads. The count losses in the reconstructed data, which are associated with high levels of activity in the bladder, produce cold area artifacts that are similar in appearance to the photon-deficient areas which are diagnostic of femoral head avascular necrosis.

and bladder disks were varied to match those of the phantom studies.

Initially the simulation study differed from the phantom measurements in the following ways:

1. The effects of the finite resolution of the gamma camera and its variation with distance from the camera face were not incorporated into the projection data calculation.
2. The effects of scatter and attenuation were not incorporated into the projection data calculation.
3. The simulated projection data were noise free.

A second simulation study was performed which attempted to reproduce some of the effects of the detection characteristics of a gamma camera. The aim was to make the simulation study more directly comparable to the phantom data. This was achieved by convolving the simulated projection data with the line spread function which was obtained from a source positioned 10 cm from the gamma camera face. To provide scatter, a block of perspex 10-cm thick was placed between the source and the camera.

A third simulation study was performed in which the attenuating effects of the other disk were incorporated into the calculation of the projection data. For this calculation, an attenuation coefficient of 0.15 cm^{-1} was used.

A square region of interest was drawn inside the center of the reconstructed bladder and femoral head disks and the counts determined in each for the set of bladder-to-femoral head count density ratios,

The exact values of the bladder-to-femoral head count density ratios are input during the projection data calculations and so do not have to be determined from planar images as was the case for the phantom studies.

RESULTS

The variation of counts in the axial sections through the femoral head phantom as a function of bladder-to-femoral head phantom activity ratios is shown in Table 1. The femoral head counts are expressed as a percentage of the counts obtained in the femoral head phantom in the study where the bladder phantom activity was zero. The counts which were observed in the axial sections through the femoral head phantom decreased as the activity in the bladder phantom increased, even though the activity in the femoral head phantom remained constant.

The variation of counts in the axial sections through the bladder phantom for the various SPECT studies is shown in Table 2. The figures are expressed as the ratio of the observed to the expected counts. The activity in each bladder phantom is known from the planar studies. This can be used, along with the counts obtained in the axial section through the least active phantom, to derive expected count values from the axial sections through each of the rest of the bladder phantoms. The counts obtained in the axial sections through the bladder phantom were consistent with the values expected from the planar measurements. The count losses observed in the sections through the femoral head phantom were not observed in the sections through the bladder phantom.

TABLE 1
Variation of Counts in Axial Sections Through the Femoral Head Phantom with the Bladder-to-Femoral Head Phantom Activity Ratio

B/F (planar)	F(axial)/F0(axial)
0	100% ± 4%
0.97	99% ± 4%
1.85	98% ± 4%
1.94	94% ± 4%
4.52	89% ± 4%
8.95	77% ± 4%
9.76	78% ± 4%
23.6	37% ± 5%
46.6	16% ± 5%

B/F (planar) is the ratio of the counts in the bladder phantom compared to the femoral head phantom as measured from the planar data.

F(axial)/F0(axial) is the femoral head phantom counts in an axial section expressed as a proportion of the counts obtained when the bladder activity was zero.

TABLE 2
Variation of Counts in the Axial Sections Through Bladder Phantom with the Bladder-to-Femoral Head Phantom Activity Ratio

B/F (planar)	OBS/EXP (axial)
0.97	100% ± 4%
1.85	98% ± 4%
1.94	101% ± 4%
4.52	96% ± 4%
8.95	100% ± 4%
9.76	102% ± 4%
23.6	105% ± 4%
46.6	103% ± 4%

B/F (planar) is the ratio of the counts in the bladder phantom compared to the femoral head phantom as measured from the planar data.

OBS/EXP (axial) is the ratio of observed to expected counts in axial sections through the bladder phantom. The expected counts were derived by multiplying the counts in the axial section through the least active bladder phantom by the relative activity in each of the rest of the phantoms which is known from the planar studies.

The results from the first simulation study are shown in Tables 3 and 4. In Table 3, the counts in the reconstructed femoral head disks are shown to increase as the count density in the bladder disk is increased. This trend is opposite to that observed from the phantom measurements.

Table 4 shows that the counts in the reconstructed bladder disk increased in proportion to the count density values used in the projection data calculation. This is consistent with the phantom measurements.

The results from the second simulation study (in which the simulated projection data were convolved with the gamma camera line spread function before reconstruction) are shown in Tables 5 and 6. In a similar manner to the first simulation study, Table 5 shows that the counts in the reconstructed femoral head disk increase as the bladder count density is increased. Again, this is opposite to the trend observed from the phantom measurements.

Table 6 shows that the counts in the reconstructed bladder disk increased in proportion to the count density values used in the projection data calculation.

The results from the third stimulation study (in which the effects of attenuation were incorporated into the projection data calculation) are shown in Tables 7 and 8. In Table 7, the counts in the reconstructed femoral head disk are shown to decrease as the count density in the bladder disk is increased. This trend is the same as that observed for the phantom measurements.

Table 8 shows that the counts in the reconstructed bladder disk increase in proportion to the count density values used in the projection data calculation.

DISCUSSION

The loss of counts in axial sections through structures in the same plane as the bladder is demonstrated by the results in Table 1. An illustration of the effects of the count loss phenomenon for the phantom studies is shown in Figure 2.

That the count losses were restricted to structures outside the bladder phantom is shown in Table 2. The counts in the axial sections through the bladder were as expected from the measurements made using the planar images.

These results imply that the count losses in the femoral head phantom were not due to some kind of arithmetic overflow during the reconstruction of the data. A further check on this was made by dividing the data in the projection images by a constant before reconstructing the SPECT study. However, no matter how large the constant value was made the count losses in the femoral head phantom were still observed. This leads to the important conclusion that it is the high dynamic range in the data

TABLE 3
Variation of Counts in the Femoral Head Disk in the Axial Section Obtained from the Reconstruction of the Simulated Projection Data with the Bladder-to-Femoral Head Count Density Ratio

B/F	F(axial)/F0(axial)
0	100%
1	100%
2	100%
5	101%
10	101%
30	112%
50	130%

B/F is the ratio of the count densities used in the calculation of the bladder and femoral head disk projection data.

F(axial)/F0(axial) is the femoral head disk counts in the axial section expressed as a proportion of the counts obtained in the section when the bladder activity was zero.

TABLE 4
Variation of Counts in the Bladder Disk in the Axial Section Obtained from the Reconstruction of the Simulated Projection Data and with the Bladder-to-Femoral Head Count Density Ratio

B/F	OBS/EXP (axial)
1	100%
2	100%
5	100%
10	100%
30	100%
50	100%

B/F is the ratio of the count densities used in the calculation of the bladder and femoral head disk projection data.

OBS/EXP (axial) is the ratio of observed to expected counts in axial sections through the bladder disk. The expected counts can be obtained by multiplying the counts in the least active bladder disk by the relative count density values used in the projection data calculations.

TABLE 5
Variation of Counts in the Femoral Head Disk in the Axial Section Obtained from the Reconstruction of the Simulated Projection Data, with the Bladder-to-Femoral Head Count Density Ratio

B/F	F(axial)/F0(axial)
0	100%
1	100%
2	100%
5	101%
10	104%
30	108%
50	112%

B/F is the ratio of the count densities used in the calculation of the bladder and femoral head disk projection data.

F(axial)/F0(axial) is the femoral head disk counts in the axial section expressed as a proportion of the counts obtained in the section when the bladder activity was zero.

The gamma camera line spread function was incorporated into the projection data simulation.

TABLE 6
Variation of Counts in the Bladder Disk in the Axial Section Obtained from the Reconstruction of the Simulated Projection Data with the Bladder-to-Femoral Head Count Density Ratio

B/F	OBS/EXP (axial)
1	100%
2	100%
5	100%
10	100%
30	100%
50	100%

B/F is the ratio of the count densities used in the calculation of the bladder and femoral head disk projection data.

OBS/EXP (axial) is the ratio of observed to expected counts in axial sections through the bladder disk. The expected counts can be obtained by multiplying the counts in the least active bladder disk by the relative count density values used in the projection data calculations.

The gamma camera line spread function was incorporated into the projection data simulation.

TABLE 8
Variation of Counts in the Bladder Disk in the Axial Section Obtained from the Reconstruction of the Simulated Projection Data with the Bladder-to-Femoral Head Count Density Ratio

B/F	OBS/EXP (axial)
1	100%
2	100%
5	100%
10	100%
30	100%
50	100%

B/F is the ratio of the count densities used in the calculation of the bladder and femoral head disk projection data.

OBS/EXP (axial) is the ratio of observed to expected counts in axial sections through the bladder disk. The expected counts can be obtained by multiplying the counts in the least active bladder disk by the relative count density values used in the projection data calculations.

The effects of attenuation were incorporated into the projection data simulation.

which causes the count losses rather than high absolute count values in the bladder phantom.

A further point to note is that the count losses could not have been caused by inconsistent data produced by activity levels which changed during the acquisition period of the study. For these phantom measurements, the activity in the bladder phantom was constant over the acquisition period.

To check that the count losses were not due to a fault or error which was specific to the particular computing system or the reconstruction algorithm used, the tests were repeated on two further systems at different sites (a Siemens Micro-delta attached to a Siemens Orbiter camera and a Link Systems Maps 2000 attached to an I.G.E 400AT). Very similar results were obtained on all systems indicating that the count loss phenomenon is probably very common.

Finally, a variety of filter functions, including the ramp filter, were used to reconstruct the data without having a significant effect on the results.

The simulation studies were performed to examine the nature of the mechanism of the count loss phenomenon. The first simulation study failed to reproduce the results of the phantom measurements. In fact as the count density in the bladder disk was increased the counts obtained in the reconstructed femoral head disk also increased (Table 3). An examination of the images obtained from the reconstructions (Fig. 3) suggests that the main cause of

TABLE 7
Variation of Counts in the Femoral Head Disk in the Axial Section Obtained from the Reconstruction of the Simulated Projection Data with the Bladder-to-Femoral Head Count Density Ratio

B/F	F(axial)/F0(axial)
0	100%
1	96%
2	91%
5	79%
10	57%
30	17%
50	12%

B/F is the ratio of the count densities used in the calculation of the bladder and femoral head disk projection data.

F(axial)/F0(axial) is the femoral head disk counts in the axial section expressed as a proportion of the counts obtained in the section when the bladder activity was zero.

The effects of attenuation were incorporated into the projection data simulation.

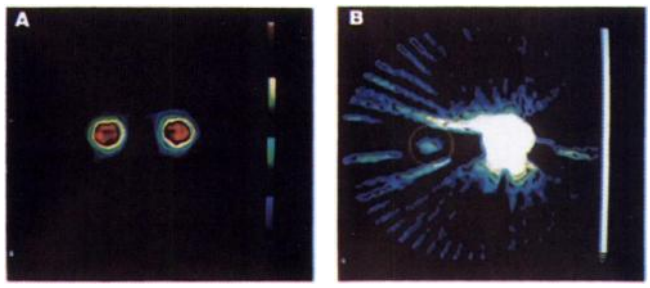

FIGURE 2. Axial sections were taken through two cylinders containing levels of activity which were chosen to represent the bladder and a femoral head. (A) Image when the activity levels were equal. (B) Image obtained when the activity in the bladder phantom was increased to 50 times that of the femoral head phantom. To help visualize the femoral head phantom, its position was delineated by a red circle and the saturation level of the color scale set to 5% of its maximum value. The counts obtained in the reconstructed femoral head phantom were only 16% of the expected value. The area within which the count losses occur is defined by lines which travel through both phantoms.

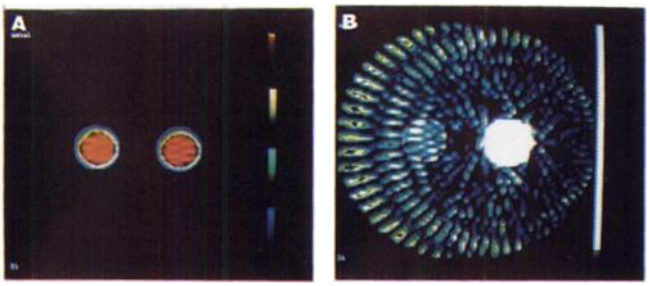

FIGURE 3. The projection data from two uniform count density disks were calculated analytically. The count densities in the disks were chosen to be the same and the projection data reconstructed (A). To simulate the effects of a high activity bladder the count density in the disk to the right was set 50 times that of the other and the data reconstructed (B). To visualize the lower activity disk, the saturation level of the color scale was set to 5% of its maximum value. The counts obtained from the lower count density disk, the position of which is delineated by the red circle, were higher than expected. This is a consequence of the angular undersampling which means that the high count projection lines through the bladder disk are not accurately cancelled out in the filtered backprojection process.

this effect is angular undersampling. In Figure 3B the projections through the bladder disk are not fully cancelled out by the back projection process in areas external to the disk itself. Although the counts in these projection lines contain only a small percentage of the bladder disk counts they can constitute a large proportion of the femoral head disk counts when the bladder-to-femoral head count density ratio is high. This was confirmed when the simulation study was repeated using 128 projection angles. The increase in counts measured in the femoral head disk was reduced from 130% to 9% when the bladder to femoral head count density ratio was 50.

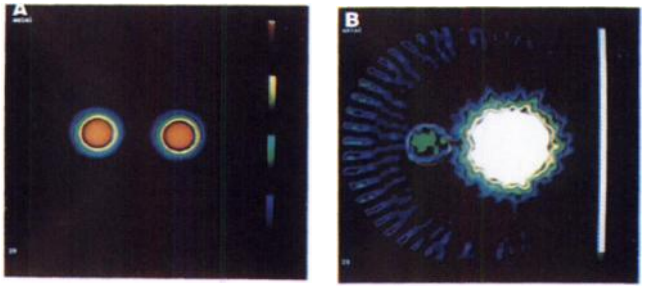

FIGURE 4. The projection data from two uniform count density disks were calculated analytically. The effects of some of the detection characteristics of the gamma camera were incorporated into the simulation by convolving the calculated projection data with a line spread function. The count densities in the disks were chosen to be the same and the projection data were reconstructed (A). To simulate the effects of a high activity bladder, the count density in the disk to the right was set to 50 times that of the other and the data reconstructed (B). To visualize the lower activity disk, the saturation level of the color scale was set to 5% of its maximum value. The counts obtained from the lower count density disk, the position of which is delineated by the red circle, were higher than expected.

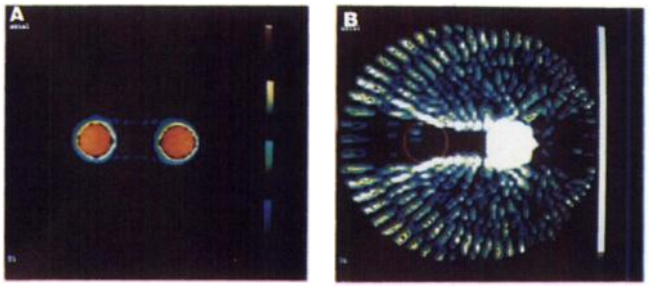

FIGURE 5. The projection data from two uniform count density disks were calculated analytically. The attenuating effects of each disk upon the other were incorporated into the calculation. The count densities in the disks were chosen to be the same and the projection data were reconstructed (A). To simulate the effects of a high activity bladder, the count density in the disk to the right was set to 50 times that of the other and the data reconstructed (B). To visualize the lower activity disk the saturation level of the color scale was set to 5% of its maximum value. The counts obtained from the lower count density disk, the position of which is delineated by the red circle, were only 12% of the expected value. The area within which the count losses occur is defined by lines which travel through both disks.

The second simulation study also failed to reproduce the results of the phantom measurements (Table 5). Compared to the first simulation study, however, the increase in femoral head counts with increasing bladder disk count density was less marked. This is a consequence of the smoothing effect of the convolution of the simulated projection data with the line spread function. The effects of this can be seen by comparing the reconstructed sections in Figure 4 with those of Figure 3.

The third simulation study successfully reproduced the count loss phenomenon observed from the phantom measurements. Table 7 shows the variation in femoral head disk counts with the count density in the bladder disk. A comparison with Table 1 shows that although the results are not exactly matched the general trend is the same. Thus, it would appear that the count loss phenomenon is a consequence, not only of the high dynamic range in the data, but also of the presence of a structure that produces a higher level of attenuation than the remainder of the objects in the reconstruction plane.

Figure 5 shows the images that were obtained from the simulation study. It can be seen from Figure 5B that the reduction in counts is located along lines which travel through both the high attenuation area and the high count area. This is a similar pattern to that observed from the phantom measurements (Fig. 1).

A consideration of the backprojection process can show how this phenomenon occurs. As no account is taken of the nonuniform attenuation within the reconstruction plane the reconstruction is performed using an inconsistent projection data set. Those points in the projection profiles which correspond to projection lines travelling through the high attenuation area will have reduced values. If the attenuating area is small and the level of nonuniform

attenuation is low, then the overall error introduced into the reconstructed data may not be significant. In clinical conditions, errors of the order of 10%, for example, can easily be obscured by noise in the data.

However, if there is also a region of high count density in the reconstruction plane then the errors in the values of the projection profile points which correspond to projection lines travelling through it and the high attenuation area can be large. In particular, these errors can constitute a significant proportion of the values of the projection profile points corresponding to projection lines which travel through only low count density structures. Thus, the reduced values obtained from the projection lines traversing both the high attenuation and the high count density regions can produce count losses in the reconstruction plane which are a significant proportion of the values in the lower count density pixels.

It should be noted that the presence of this form of artifact is not restricted to SPECT bone studies of the pelvis. It can occur in any SPECT study in which a high count density area and a high attenuation area are present in the reconstruction plane. For example, count losses in the spine (the high attenuation area) have been observed when a high level of activity is present in the renal pelvis (*2*).

If the presence of a count loss artifact is suspected there are a number of methods which can be used to correct for it. The replacement of the counts in the bladder by data that are as representative as possible of the activity in the surrounding structures can be made by using a linear or a bilinear interpolation scheme (*3,4*). By defining a single region of interest on the sinogram corresponding to the section through the center of the bladder, the position of the bladder in all 64 projection images can be automatically determined. This means that the correction procedure can be implemented rapidly (i.e., in less than 1 min).

A different approach which uses a truncation of the high counts in the bladder has also been suggested (*2*). The high success rate reported for the removal of the cold area artifacts was similar to that obtained from the interpolation procedures (*5*).

An alternative approach which is suggested from the results of the simulation studies would be to correct for the effects of the nonuniform attenuation within the reconstruction plane.

CONCLUSIONS

Using some simple phantom studies, the count loss phenomenon observed in clinical SPECT imaging has been reproduced. From these studies, it was found that the count losses are independent of the filter used to reconstruct the data. It was also shown that they are not a consequence of changes in activity levels during the acquisition period of the study. Lastly, it was demonstrated that the errors are not due to arithmetic overflows in the backprojection calculation. The projection data can be divided by an arbitrary constant value without affecting the results.

To examine the nature of the mechanism of the count loss phenomenon in more detail a set of simulation studies were performed. It was found that the results of the phantom studies could only be reproduced if the effects of photon attenuation were incorporated into the projection data calculations. This leads to the conclusion that it is the combination of the presence of both a high count density region and a high attenuation structure that cause the count losses. The reduction in counts produced by the additional attenuation of projection lines which pass through both the high count density area and the high attenuation area can be large in proportion to the count values of the projection lines in the remainder of the reconstruction plane. Thus, when the reconstruction is performed significant errors in the count values of the lower count density structures can occur. The pattern of the count loss phenomenon observed in both the phantom and the simulation studies is also consistent with this explanation. The area of reduced counts is located in the region of the axial plane that is defined by lines which pass through both the high count density area and the high attenuation structure.

Finally, an awareness of the combination of circumstances that can lead to the production of cold area artifacts in SPECT imaging can be used to decide when one of the available correction methods should be applied.

REFERENCES

1. Collier BD, Carrerra GF, Johnson RP, et al. Detection of femoral head avascular necrosis in adults by spect. *J Nucl Med* 1985;26:979–987.
2. Bunker SR, Handmaker H, Torre MT, Schmidt WP. Pixel overflow artifacts in SPECT evaluation of the skeleton. *Radiology* 1990;174:229–232.
3. Gillen GJ, McKillop JH, Hilditch TE, Davidson JK, Elliott AT. Digital filtering of the bladder from SPECT bone studies of the pelvis. *J Nucl Med* 1988;29:1587–1595.
4. Kouris K, Musa A, Taha B, Abdel-Dayem HM, Collier BD. Correction of the bladder artifact in hip SPECT [Abstract]. *J Nucl Med* 1988;29:868.
5. O'Connor MK, Kelly BJ. Evaluation of techniques for the elimination of "hot" bladder artifacts in SPECT of the pelvis. *J Nucl Med* 1990;31:1872–1875.